Biomedicine & Pharmacotherapy 159 (2023) 114220

Contents lists available at ScienceDirect

Biomedicine & Pharmacotherapy

journal homepage: www.elsevier.com/locate/biopha

PBMCs gene expression signature of advanced cirrhosis with high risk for clinically significant portal hypertension in HIV/HCV coinfected patients: A cross-control study

Sergio Salgüero [a,b,1], Óscar Brochado-Kith [a,c,1], Ana Virseda Verdices [a,c,1], Juan Berenguer [c,d,e], Juan González-García [c,f,g], Isidoro Martínez [a,c], Cristina Díez [c,d,e], Víctor Hontañón [c,f,g], Leire Pérez-Latorre [c,d,e], Amanda Fernández-Rodríguez [a,c,1], María Ángeles Jiménez-Sousa [a,c,*,1], Salvador Resino [a,c,*,1]

[a] Unidad de Infección Viral e Inmunidad, Centro Nacional de Microbiología, Instituto de Salud Carlos III, Majadahonda, Madrid, Spain
[b] Unidad de Análisis Clínicos, Hospital El Escorial, Spain
[c] Centro de Investigación Biomédica en Red de Enfermedades Infecciosas (CIBERINFEC), Instituto de Salud Carlos III, Madrid, Spain
[d] Unidad de Enfermedades Infecciosas/VIH; Hospital General Universitario "Gregorio Marañón", Madrid, Spain
[e] Instituto de Investigación Sanitaria del Gregorio Marañón, Madrid, Spain
[f] Unidad de VIH; Servicio de Medicina Interna, Hospital Universitario "La Paz", Madrid, Spain
[g] Instituto de Investigación Sanitaria La Paz (IdiPAZ), Madrid, Spain

ARTICLE INFO

Keywords:
HIV/HCV coinfection
Gene expression
RNA-seq
PBMCs
Liver stiffness
Advanced cirrhosis

ABSTRACT

Background: Patients with advanced cirrhosis are at high risk of developing clinically significant portal hypertension (CSPH). We analyzed the gene expression profile of peripheral blood mononuclear cells (PBMCs) from HIV/HCV coinfected patients to identify a gene expression signature of advanced cirrhosis with high risk for CSPH.

Methods: We conducted a cross-sectional study on 68 patients. Liver stiffness measurement (LSM) was used to stratify patients into < 12.5 kPa (no cirrhosis, n = 19), 12.5 – 24.9 kPa (cirrhosis, n = 20), and ≥ 25 kPa (advanced cirrhosis with high risk for CSPH, n = 29). Besides, we further evaluated LSM < 25 kPa (n = 39) vs. ≥ 25 kPa (n = 29). Total RNA was extracted from PBMCs, and poly(A) RNA sequencing was performed. Two significant differentially expressed (SDE) transcripts were validated by quantitative PCR in a different cohort (n = 46).

Results: We found 60 SDE transcripts between patients with LSM < 12.5 kPa and ≥ 25 kPa. Partial least squares discriminant analysis showed that those 60 SDE transcripts collectively discriminated LSM ≥ 25 kPa, with an area under the receiver operating characteristic curve (AUROC) of 0.84. Eight genes had an AUROC ≥ 0.75 for LSM ≥ 25 kPa: five were positively associated with LSM values (*SCAMP1, ABHD17B, GPR146, GTF2A1,* and *TMEM64*), while three were inversely associated (*ZFHX2-AS1*, *MDK*, and *STAG3L2*). We validated the two SDE

Abbreviations: HIV, Human immunodeficiency virus; HCV, Hepatitis C virus; HCC, Hepatocellular carcinoma; LSM, Liver stiffness measurement; kPa, Kilopascals; CSPH, Clinically significant portal hypertension; PBMCs, Peripheral blood mononuclear cells; cART, Combination antiretroviral therapy; RIN, RNA integrity number; TMM, Trimmed mean of the M-values; RT-qPCR, Reverse transcription-quantitative PCR; MDK, Midkine; STAG3L2, Stromal antigen 3-like 2; GLM, Generalized linear models; FC, Fold-change; FDR, False discovery rate; SDE, Significantly differentially expressed; AMR, Arithmetic mean ratio; PLS-DA, Partial least squares discriminant analysis; AUROC, Area under the ROC curve; SCAMP1, Secretory carrier membrane protein 1; ABHD17B, Abhydrolase domain containing 17B; GPR146, G protein-coupled receptor 146; GTF2A1, General transcription factor IIA subunit 1; TMEM64, Transmembrane protein 64; ZFHX2-AS1, Zinc finger homeobox 2 antisense RNA 1; SERCA, Sarcoendoplasmic reticulum Ca2 + ATPase; HPVG, Hepatic venous pressure gradient measurement.

* Correspondence to: Centro Nacional de Microbiología, Instituto de Salud Carlos III (Campus Majadahonda), Carretera Majadahonda, Pozuelo, Km 2.2, Majadahonda, 28220 Madrid, Spain.

E-mail addresses: sergio.salguero@salud.madrid.org (S. Salgüero), obrochado@isciii.es (Ó. Brochado-Kith), virseda.ana@gmail.com (A.V. Verdices), jbb4@me.com (J. Berenguer), juangonzalezgar@gmail.com (J. González-García), imago@isciii.es (I. Martínez), crispu82@gmail.com (C. Díez), victor.hontanon@gmail.com (V. Hontañón), legor78@hotmail.com (L. Pérez-Latorre), amandafr@isciii.es (A. Fernández-Rodríguez), jimenezsousa@isciii.es (M.Á. Jiménez-Sousa), sresino@isciii.es (S. Resino).

[1] These authors contributed equally to this work.

https://doi.org/10.1016/j.biopha.2023.114220
Received 9 November 2022; Received in revised form 3 January 2023; Accepted 4 January 2023
Available online 9 January 2023

transcripts with the highest discrimination capacity in a different cohort, finding significant differences between < 25 kPa and ≥ 25 kPa (*MDK* ($p = 0.006$) and *STAG3L2* ($p = 0.021$)).
Conclusions: A gene expression signature of 60 transcripts was associated with advanced cirrhosis with high risk for CSPH in HIV/HCV coinfected patients.

1. Background

Both human immunodeficiency virus (HIV) and hepatitis C virus (HCV) share transmission routes, cause chronic infections, and represent a significant global health burden [1]. HIV/HCV coinfection is common, and liver disease is the leading cause of morbidity and mortality among coinfected patients [2]. HIV/HCV-coinfected patients develop cirrhosis more rapidly than their HCV monoinfected counterparts [3], with higher rates of liver decompensation, end-stage liver disease, hepatocellular carcinoma (HCC), and liver-related death [4].

Liver fibrosis is a dynamic response to liver injury that leads to the accumulation of extracellular matrix. When the damage is maintained, the liver parenchyma is gradually replaced by scar tissue, which can lead to cirrhosis [5]. Chronic hepatitis C promotes massive destruction of hepatocytes, leading to significant pathophysiological changes during advanced fibrosis and cirrhosis [6], such as immune activation, inflammation, and coagulopathy [7], which can trigger the appearance of cirrhosis-associated immune dysfunction, characterized by systemic inflammation and immune deficiency [8]. These pathophysiological processes contribute to an increased risk of infections, organ failure [8], and carcinogenesis [9]. After HCV eradication, epigenetic and immunological alterations persist [10], and the burden of liver cirrhosis remains substantial for a long time [11]. In addition, HIV/HCV-coinfected patients continue to have a higher mortality risk than HCV-monoinfected patients [12].

An accurate assessment of the degree of liver fibrosis is a crucial step for proper patient management. A widely used physical method to assess liver fibrosis is using transient elastography (Fibroscan®), which reports liver stiffness measurement (LSM) in kilopascals (kPa) to estimate liver fibrosis [13]. In this regard, LSM ≥ 12.5 kPa is considered cirrhosis [13], and ≥ 25 Kpa is advanced cirrhosis with high risk for clinically significant portal hypertension (CSPH) [14,15].

Liquid biopsy, such as a blood sample, can overcome the limitations of both liver biopsy and current noninvasive methods [16]. Peripheral blood mononuclear cells (PBMCs), one of the main extrahepatic reservoirs of HCV, may be an excellent source of biomarkers reflecting HCV liver infection [17,18]. There is a continuing interest in developing new biomarkers that support clinical decisions. The application of omics techniques has opened multiple possibilities to identify suitable biomarkers for liver fibrosis, which has already been applied in the context of viral hepatitis [19,20]. Furthermore, using transcriptomics can help us elucidate the molecular mechanisms behind liver fibrosis at different stages [21] and the acceleration of liver disease in HIV/HCV-coinfected patients [22]. Identifying key molecular cues in liver fibrosis can accelerate the development of antifibrotic agents to reverse persistent hepatic pathology after HCV eradication [16,23]. These approaches should be applied to accessible tissues to identify non-invasive biomarkers.

1.1. Objective

We aimed to analyze the gene expression profile of PBMCs in HIV/HCV coinfected patients with different degrees of fibrosis/cirrhosis, measured by LSM using transient elastography, to identify a gene expression signature of advanced cirrhosis with high risk for CSPH in this population group.

2. Methods

2.1. Patients

We conducted a cross-sectional study on 68 HIV/HCV-coinfected patients (training cohort) and 46 HIV/HCV-coinfected patients (validation cohort). For this study, inclusion criteria were: 1) detectable HCV-RNA (HCV+) and HIV-DNA (HIV+) in peripheral blood by polymerase chain reaction; 2) LSM data available; 3) PBMCs sample available; 4) combination antiretroviral therapy (cART) for at least six months or no need for cART according to guidelines used in the study period; 5) $CD4^+$ T cell ≥ 200 cells/μL; 6) undetectable plasma HIV-RNA viral load (<50 copies/mL). Patients with acute hepatitis C, hepatitis B virus coinfection, and previous diagnosis of HCC were excluded.

Data and samples were selected from two previously described cohorts: GESIDA 3603b cohort (November 2012 and February 2014, n = 63) and the ESCORIAL cohort (March 2015 and September 2015, n = 51) (Appendix) [24,25]. Both cohorts belong to specific research projects approved by the Research Ethics Committee of the Instituto de Salud Carlos III (References CEI PI 23_2011 and CEI PI 41_2014, respectively), which verify the ethical development of research projects. The study was conducted according to the Declaration of Helsinki, and all participants gave their written consent before enrollment.

2.2. Clinical data and samples

Clinical data were collected using an online form, and the information was monitored. As previously described, trained operators assessed LSM using transient elastography (FibroScan®, Echosens, Paris, France) [7]. The LSM ranged from 2.5 to 75 kPa.

Clinical samples were obtained by venipuncture in ethylenediaminetetraacetic acid tubes. Peripheral venous blood samples were sent to the HIV HGM BioBank (http://hivhgmbiobank.com/?lang=en) on the same day of the extraction. PBMCs were isolated by Ficoll-Paque density gradient and stored in liquid nitrogen (−180 °C) until use.

2.3. Outcome variables

The outcome variable was LSM (kPa), using the following strata [13–15]: i) < 12.5 kPa (no cirrhosis); ii) 12.5 – 24.9 kPa (cirrhosis), and iii) ≥ 25 kPa (advanced cirrhosis with high risk for CSPH, Baveno VII Consensus Workshop)). In addition, we assessed the presence of LSM $\geq$ 25 kPa.

2.4. RNA extraction, library preparation, and RNA sequencing

According to the manufacturer's instructions, total RNA was extracted from PBMCs using the RNeasy Micro kit (Qiagen, Hilden, Germany). RNA concentration was quantified using NanoDrop 2000 Spectrophotometer (ThermoFisher). The RNA quality was evaluated by the RNA Integrity Number (RIN) using 2100 Bioanalyzer RNA Nano assay (Agilent). Only samples with RIN > 7.5 were selected for library preparation.

Libraries were synthesized following Illumina's TruSeq Stranded mRNA Sample Prep Kit v2 protocol, using 500 nanograms of total RNA of each sample. With this procedure, polyadenylated RNAs were captured, including coding RNA and multiple forms of noncoding polyadenylated RNAs. Next, libraries were pooled for multiplexed sequencing to obtain an average of 25 million reads per sample.

Sequencing was then performed on an Illumina HiSeq2500, single read, 50nts (1 ×50). Library preparation and sequencing were performed at the Centre for Genomic Regulation in Barcelona (Spain). More details on these processes were recently described by our group [26]. The raw sequencing data were processed using FastQC (v. 0.11.8) for quality control and Trimmomatic (v. 0.38) for adapter trimming. The applied bioinformatics workflow includes sequence alignment with STAR (v. 2.6.1d), using GRCh38 as a reference genome, and the Subread's featureCounts software (v. 1.6.4) for reading count extraction [26]. The raw RNA-seq data are publicly available at the ArrayExpress repository (EMBL-EBI; https://www.ebi.ac.uk/) under the accession number E-MTAB-12251.

Before testing for differentially expressed transcripts, filtering and normalization were applied to RNA-Seq data with the *edgeR* package (v. 3.32.1). Briefly, transcripts with low counts were first filtered out using the *filterByExpr()* function. Normalization was then performed by applying the trimmed mean of the M-values (TMM) method.

2.5. Quantitative Reverse Transcription PCR (RT-qPCR)

RT-qPCR was used to validate the expression of differentially expressed genes by RNA sequencing. Total RNA previously extracted was reverse-transcribed with the High-Capacity cDNA Reverse Transcription Kit (Applied Biosystems) according to the manufacturer's protocol. Generated cDNA was used to quantify the expression of the selected genes by RT-qPCR using Taqman Gene Expression Assays (FAM dye-labeled, Applied Biosystems) specific for each gene in a Step One system (Applied Biosystems). PCRs were run in triplicate for *midkine (neurite growth-promoting factor 2)* (*MDK*; Hs00171064_m1) and *stromal antigen 3-like 2* (*STAG3L2*; Hs00414793_m1) genes. To normalize the quantification of an mRNA target for differences in the amount of total RNA, we used *actin-β* (ACTB; Hs99999903_m1) as an endogenous control.

We performed a relative quantification using the comparative Ct (ΔΔCt) method (Applied Biosystems User Bulletin no. 2) using a random mixture of samples from six HIV-infected patients as a reference sample (calibrator). Quantifying target mRNA expression was performed relative to the calibrator, expressed as n-fold for all samples.

2.6. Sample size calculation

The sample size was calculated according to the RNASeqPower package (v. 1.30.0), using 25 million reads per sample, a minimum fold change of 1.5, an alpha of 0.05, and an estimated dispersion of 0.4. For pairwise comparison of the strata of cirrhosis according to LSM (< 12.5 kPa (n = 19), 12.5 – 24.9 kPa (n = 20), and ≥ 25 kPa (n = 29)), we found a statistical power of 0.82 when comparing groups of at least 20 patients each. For comparison of advanced cirrhosis with high risk for CSPH (<25 kPa (n = 39) vs. ≥ 25 kPa (n = 29)), we found a statistical power of 0.96.

2.7. Statistical analysis

All statistical analyses were performed using R version 3.6.1 (R Foundation for Statistical Computing, Vienna, Austria), Stata/IC 17 (StataCorp, Texas, USA), and GraphPad Prism 7.04 (GraphPad Software, Inc., California, USA). All *p*-values were two-tailed, and statistical significance was set as $p \leq 0.05$.

A descriptive analysis of the study population was performed by applying the Chi-squared or Fisher's exact test on categorical variables and the Kruskal-Wallis test on continuous variables.

For gene expression analysis, we analyzed the differences in gene expression in PBMCs (counts per million) between all possible pairwise comparisons among patient groups according to LSM strata (< 12.5kPa, 12.5 - 25 kPa, ≥ 25 kPa), using generalized linear models (GLM) with a negative binomial distribution (*stats* package v3.6.2 in R). The GLM test provides the fold-change (FC) and its level of significance (*p*-value), which were corrected for multiple tests using the false discovery rate (FDR) with the Benjamini and Hochberg method (*q*-value). Transcripts with FC ≥ 1.5 in both directions and a *q*-value ≤ 0.05 were considered significantly differentially expressed (SDE). Besides, the linear association between SDE genes (counts per million) and LSM (kPa) as a continuous variable was also evaluated. This test provides the arithmetic mean ratio (AMR) and the 95% confidence interval (95%CI). Marginal effects were computed, and results were plotted using the ggpredict function from the *ggeffects* package. Next, we evaluated the discriminatory performance of the SDE transcripts resulting from GLMs to distinguish advanced cirrhosis with high risk for CSPH (< 25 kPa vs. ≥ 25 kPa).

We also carried out a supervised multivariate analysis (multiple dependent variables) with the SDE transcripts previously identified to confirm patients' clusterization using a partial least squares discriminant analysis (PLS-DA) [R-packages *mixOmics v6.3.2*]. PLS-DA creates a regression model that classifies patients based on all SDE transcripts, dealing with common multicollinearity among transcripts. This test gives us the area under the receiver operating characteristic curve (AUROC) of all SDE transcripts (cirrhosis signature) for discriminating advanced cirrhosis with high risk for CSPH (< 25 kPa vs. ≥ 25 kPa), considering that an AUROC between 0.90 and 1 was outstanding, 0.80–0.90 was excellent, and 0.70–0.80 was good. We also analyzed the discriminatory performance of each SDE transcript separately to discriminate advanced cirrhosis with high risk for CSPH (< 25 kPa vs. ≥ 25 kPa) via AUROC calculation.

3. Results

3.1. Significant differences between fibrosis strata

Characteristics of HIV/HCV-coinfected patients (training cohort) were similar among LSM strata (Table 1), except for nadir $CD4^+$ T-cells ($p = 0.017$), LSM ($p < 0.001$), and total cholesterol levels ($p = 0.005$).

RNA-seq samples showed an average of 23.47 million reads and 99.04% mapped to the reference genome. A total of 60,623 different genes were identified, but only 15,642 met the filtering criteria for subsequent analysis (see methods).

No significant differences were observed among contiguous fibrosis strata (< 12.5kPa vs. 12.5 kPa-24.9 kPa, and 12.5 kPa-24.9 kPa vs. ≥ 25 kPa; *q*-value > 0.25). However, a total of 60 SDE transcripts were found between patients with extreme LSM values, LSM < 12.5 kPa (no cirrhosis) vs. LSM ≥ 25 kPa (advanced cirrhosis with high risk for CSPH) (Fig. 1; the full description is in Supplementary Table 1). Twenty-two out of 60 SDE genes were downregulated, and 38 were upregulated in patients with advanced cirrhosis with high risk for CSPH. Additionally, these 60 SDE transcripts followed a significant linear association with LSM values in all cases, whether positive or negative (Supplementary Table 2 and Supplementary Figure 1). We used these 60 SDE transcripts for further analyses.

3.2. Gene expression discriminates advanced cirrhosis with high risk for CSPH

Subsequently, we stratified all HIV/HCV patients of the training cohort into two groups by absence (< 25 kPa) or presence (≥ 25 kPa) of advanced cirrhosis with high risk for CSPH. Clinical, epidemiological, and virological characteristics are displayed in Supplementary Table 3. Patients with ≥ 25 kPa had lower values of total cholesterol ($p = 0.001$), LDL ($p = 0.037$), and HDL ($p = 0.030$).

PLS-DA showed that the previous 60 SDE transcripts collectively discriminated between patients with and without advanced cirrhosis with high risk for CSPH (AUROC = 0.835) (Fig. 2A), with an excellent discrimination ability (AUROC = 0.84; Fig. 2B). Moreover, we individually assessed this ability for each of the 60 SDE transcripts previously

Table 1
Clinical, epidemiological, and virological characteristics of HIV/HCV-coinfected patients in training set according to values of LSM.

	All	< 12.5 kPa	12.5 – 24.9 kPa	≥ 25 kPa	*p*-value
No.	68	19	20	29	
Gender (male)	48 (70.6%)	12 (63.2%)	15 (75%)	21 (72.4%)	0.691
Age (years)	50.5 (47; 53)	50.4 (45; 53)	48.4 (46.3; 53.1)	50.9 (48.7; 53.6)	0.513
BMI (kg/m^2) (n = 65)	23.8 (21.7; 25.5)	23.6 (20.4;26.4)	24.1 (22.9; 25.2)	23.3 (21.7; 25.7)	0.798
BMI ≥ 25 (kg/m^2) (n = 65)	21 (32.3%)	7 (38.9%)	5 (26.3%)	9 (32.1%)	0.716
Alcohol consumed ever	36 (52.9%)	8 (42.1%)	11 (55%)	17 (58.6%)	0.521
Intravenous drug user	57 (83.8%)	16 (84.2%)	16 (80%)	25 (86.2%)	0.844
Previous HCV therapy	30 (44.1%)	7 (36.8%)	13 (65%)	10 (34.5%)	0.081
HIV antiretroviral therapy					0.349
NRTI + II-based	29 (42.6%)	8 (42.1%)	7 (35%)	14 (48.3%)	
NRTI + NNRTI-based	11 (16.2%)	4 (21.1%)	5 (25%)	2 (6.9%)	
NRTI + PI-based	6 (8.8%)	2 (10.5%)	1 (5%)	4 (13.8%)	
PI-based	7 (10.3%)	2 (10.5%)	3 (15%)	2 (6.9%)	
PI + II-based	4 (5.9%)	2 (10.5%)	2 (10%)	0 (0%)	
Others	10 (14.7%)	1 (5.3%)	2 (10%)	7 (24.1%)	
HIV markers					
Nadir CD4$^+$ T-cells (n = 67)	122 (71; 224)	234 (70; 367)	88 (52.5; 172.5)	114.7 (93.5; 180)	**0.017**
CD4$^+$ T-cells/mm^3	520.5 (279.5; 822.5)	695 (455; 814)	370.5 (245; 760.2)	434 (236.5; 901.5)	0.404
HCV markers					
HCV genotype (n = 66)					0.349
1	40 (60.6%)	11 (57.9%)	14 (70%)	15 (55.6%)	
2	1 (1.5%)	0 (0%)	0 (0%)	1 (3.7%)	
3	15 (22.7%)	7 (36.8%)	2 (10%)	6 (22.2%)	
4	10 (15.2%)	1 (5.3%)	4 (20%)	5 (18.5%)	
Log$_{10}$ HCV-RNA (IU/mL)	6.4 (5.8; 6.6)	6.4 (5.9; 6.8)	6.2 (5.5; 6.5)	6.4 (5.9; 6.7)	0.187
HCV-RNA > 850.000 IU/mL	48 (70.6%)	13 (68.4%)	13 (65%)	22 (75.9%)	0.693
LSM (Kpa)	21 (11.9; 34.6)	9.8 (7.8; 11.4)	17.6 (14.8; 21.1)	36.3 (27.3; 40.6)	**< 0.001**
Biochemical markers					
Triglycerides (mg/dL)	114 (79; 161)	106 (65.5; 182.5)	115 (80; 160)	115 (81; 183)	0.781
Total cholesterol (mg/dL)	151 (123; 174)	167 (136; 193)	169.5 (129.5; 194.7)	130.5 (105.5; 156.5)	**0.005**
LDL (mg/dL)	74.5 (56; 104)	94 (57.5; 108)	93 (65; 108.2)	60 (53.5; 84)	0.113
HDL (mg/dL)	44.5 (34; 58)	48 (34; 61)	51 (40; 58)	37 (29.5; 50.5)	0.089

Statistics: The values are expressed as the absolute number (percentage) and median (interquartile range). P-values were calculated by the Fisher's exact test and the Kruskal-Wallis test.
Abbreviations: BMI, body mass index; HCV, hepatitis C virus; HIV, human immunodeficiency virus; NRTI, nucleoside analogue HIV reverse transcriptase inhibitor; II, HIV integrase inhibitor; NNRTI, non-nucleoside analogue HIV reverse transcriptase inhibitor; PI, HIV protease inhibitor; LSM, liver stiffness measurement; HCV-RNA, viral load of hepatitis C; HDL, high-density lipoprotein; LDL, low-density lipoprotein.

identified (Supplementary Table 4). We found eight genes with an AUROC ≥ 0.75 (Table 2). Five out of 8 genes were positively associated with LSM values: *secretory carrier membrane protein 1 (SCAMP1), abhydrolase domain containing 17B (ABHD17B), general transcription factor IIA subunit 1 (GTF2A1), transmembrane protein 64 (TMEM64)*, and *G protein-coupled receptor 146 (GPR146)*; while three genes were negatively associated: *zinc finger homeobox 2 antisense RNA 1 (ZFHX2-AS1)*, *MDK*, and *STAG3L2*.

3.3. SDE transcripts validation

RT-qPCR was used to confirm the significance of the two SDE transcripts with higher discrimination ability for advanced cirrhosis with high risk for CSPH (*STAG3L2* and *MDK*) in a validation cohort of 46 HIV/HCV-coinfected patients (Supplementary Table 5) with similar characteristics to the training cohort. Both *MDK* ($p = 0.006$; Fig. 3A) and *STAG3L2* ($p = 0.021$; Fig. 3B) showed significant differences between < 25 kPa and ≥ 25 kPa groups.

4. Discussion

We found a PBMCs gene expression signature of 60 SDE transcripts in HIV/HCV coinfected patients between extreme phenotypes of cirrhosis (non-cirrhotic (< 12.5 kPa) vs. advanced cirrhosis with high risk for CSPH (≥ 25 kPa)). Assessing PBMCs expression is a worthy option since it may resemble some molecular mechanism related to HCV in the liver [16,18]. Besides, most gene expression changes overlap between the liver and PBMCs compartments in coinfected patients, supporting the systemic nature of inflammatory cues [27]. Lastly, the immune system is a critical element in the pathogenesis of liver fibrosis [5]. PBMCs may be arguably the best tissue to assess the chronic inflammatory state during chronic hepatitis, acting as an interplay between the liver and systemic factors. Therefore, our results may reflect the relationship between the state of the immunological system and the cirrhotic stage. In this regard, transcriptomics has already been applied to PBMCs to gain insight into immune system activity in the context of different liver diseases [28]. However, both HCV and HIV can infect PBMCs and, thus, alter their expression, making studies in HIV/HCV-coinfected patients necessary.

Our study did not find differences in contiguous fibrosis stages (<12.5 kPa vs. 12.5 – 24.9 kPa and 12.5 – 24.9 kPa vs. ≥ 25 kPa), probably because changes in gene expression are gradually established as fibrosis increases, and our statistical power is limited to detect them. However, we found a set of 60 SDE transcripts when groups with extreme LSM values (< 12.5 kPa vs. ≥ 25 kPa) were compared, as differences were maximized. Of note, an increased number of lncRNAs (e.g., *AD000090.1*) or pseudogenes (e.g., *TPT1P9*) were significantly altered, supporting the growing evidence that noncoding RNAs are critical key players during liver cirrhosis progression [29].

We analyzed these 60 SDE transcripts to discriminate the CSPH (< 25 kPa vs. ≥ 25 kPa). Collectively, this set of transcripts was able to correctly classify patients with advanced cirrhosis with high risk for CSPH. Eight of them showed good independent discriminatory performance (AUROC ≥ 0.75). The expression values of five of these transcripts were positively associated with LSM (*SCAMP1, ABHD17B, GPR146, GTF2A1,* and *TMEM64*). Some of these overexpressed genes have already been involved in HCC (*GTF2A1, SCAMP1*, and *TMEM64*). *GTF2A1* has previously been found to play a role in HCC [30]. *GTF2A1* encodes the general transcription factor IIA subunit 1, which, together with *GTF2A2*, forms the general transcriptional regulator TFIIA, which is regulated through multiple complex regulatory mechanisms,

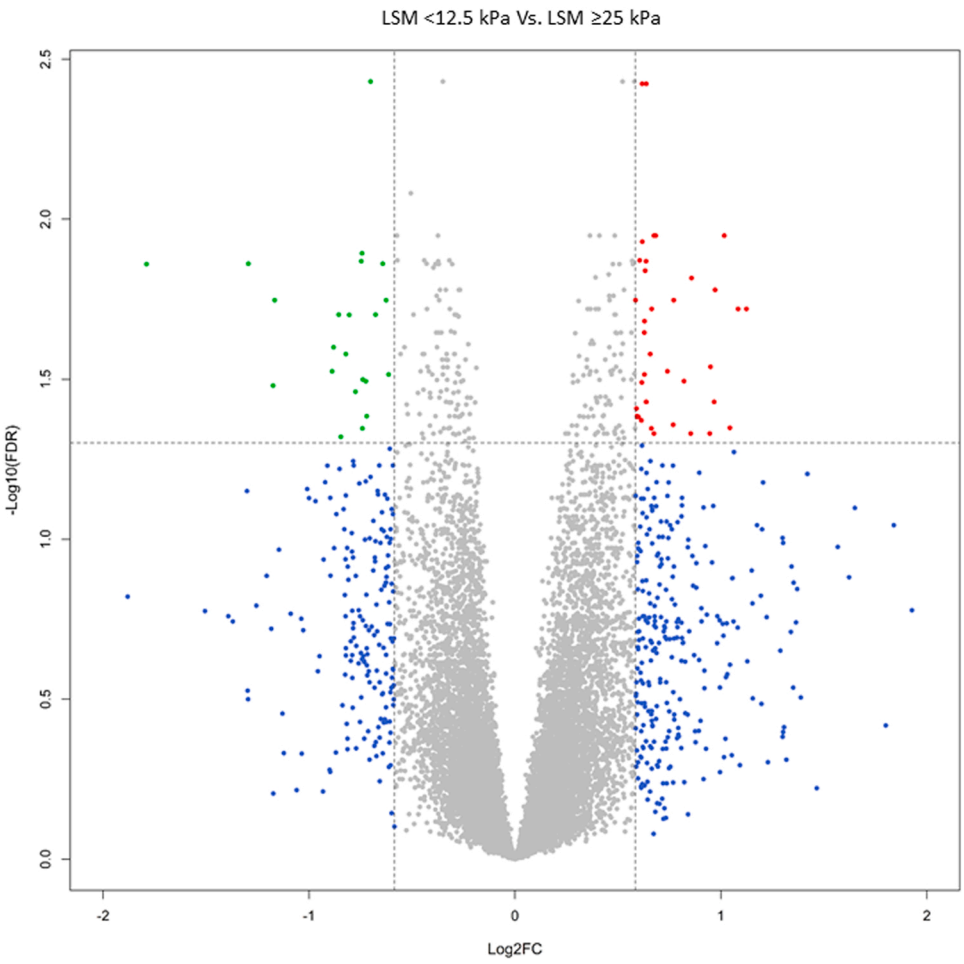

Fig. 1. Volcano plot of the differences in gene expression in PBMCs from HIV/HCV coinfected patients clustered according to LSM < 12.5 kPa (no cirrhosis) versus LSM ≥ 25 kPa (high risk for clinically significant portal hypertension, CSPH). Significant upregulated and down-regulated transcripts are illustrated as red and green circles, respectively. Statistics: The volcano plot is depicted with the fold change (FC) of each transcript calculated by the GLM test. The significance level was corrected for multiple testing using the false discovery rate (FDR) with the Benjamini and Hochberg method. Abbreviations: FC, Fold-change; FDR, False discovery rate.

including site-specific proteolysis by the highly conserved protease Taspase 1 [31]. Taspase 1 overexpression has already been associated with HCC [32]. SCAMP1 is a protein involved in the endomembrane system and vesicle trafficking[33], and its dysregulation may contribute to several diseases, such as cancer [34]. Extracellular vesicles, especially exosomes, are the main form of communication in the liver [35], and HCV and HIV are known to hijack the host exosomal machinery. While each SCAMP member may have a distinctive role in trafficking pathways [33], it is worth mentioning that another member of the same family, *SCAMP3*, has already been related to the pathogenesis of HCC [36]. *TMEM64*, which has already been associated with HCC [37], codes for a transmembrane protein capable of modulating Wnt signaling, which in turn may be involved in promoting liver fibrosis [38] and the development of HCC [39]. In addition, *TMEM64* positively mediates sarcoendoplasmic reticulum Ca^{2+} ATPase (SERCA) activity [40], a critical regulator of calcium homeostasis and signaling, which regulates Th17 cell differentiation [41]. This would agree with previous findings in which HIV/HCV-coinfected patients with higher degrees of cirrhosis (LSM ≥ 25 kPa) had the lowest plasma cytokine values related to Th17 response [42].

The remaining overexpressed genes in patients with advanced cirrhosis with high risk for CSPH, *GPR146,* and *ABHD17B*, together with the previously commented *TMEM64,* could also be related to metabolic function. HIV and HCV infections cause alterations in metabolism, which triggers a pathological process that leads to liver steatosis and cirrhosis [43]. *GPR146* has been given a role in the selective inhibition of RNA virus infection [44], exerts a detrimental effect on the regulation of systemic cholesterol metabolism [45], and, therefore, its overexpression could contribute to the alteration of lipid metabolism. This would agree with the lower cholesterol values detected in our patients with LSM ≥ 25 kPa. *TMEM64* overexpression has been associated with increased adipogenesis [46], and *ARL15*, another SDE overexpressed in patients with LSM ≥ 25 kPa, may predispose them to lipodystrophy [47]. *ABHD17B* codes for an enzyme with depalmitoylating activity. Palmitoylation alterations have been associated with different neurological disorders [48], which could explain the neurological manifestations often described in HCV-infected patients with LSM ≥ 25 kPa [49]. Besides, *ABHD17B* appears to be involved in progressing from cirrhosis to HCC [50]. The *ABHD17B* overexpression detected in our study is consistent with previous findings, where higher free fatty acids and glycerol levels in patients with higher Child-Turcotte-Pugh scores were found [51].

On the other hand, three additional transcripts showed good discriminatory performance (*STAG3L2*, *MDK*, and *ZFHX2-AS1*), whose expression decreased with LSM values. *ZFHX2-AS1* is a lncRNA without known function besides the putative negative regulator of the transcription factor *ZFHX2,* promoting upregulation of somatostatin [52], which is elevated in cirrhotic patients [53]. These results support our current findings, where the down-regulation of *ZFHX2-AS1* contributes to advanced cirrhosis with high risk for CSPH. *STAG3L2* is a pseudogene of unknown function, predicted to be involved in chromatin dynamics, according to the Alliance of Genome Resources (Apr 2022). *STAG3L2* shows low expression values in the average adult liver [54]; conversely, it is highly expressed in the liver of HCC patients [55]. *MDK* encodes for midkine, a heparin-binding growth factor that has pro-inflammatory, angiogenic, and anti-apoptotic functions implicated in several inflammatory pathophysiological processes, such as autoimmune disease and cancer [56]. The presence of high levels of MDK in serum is a promising

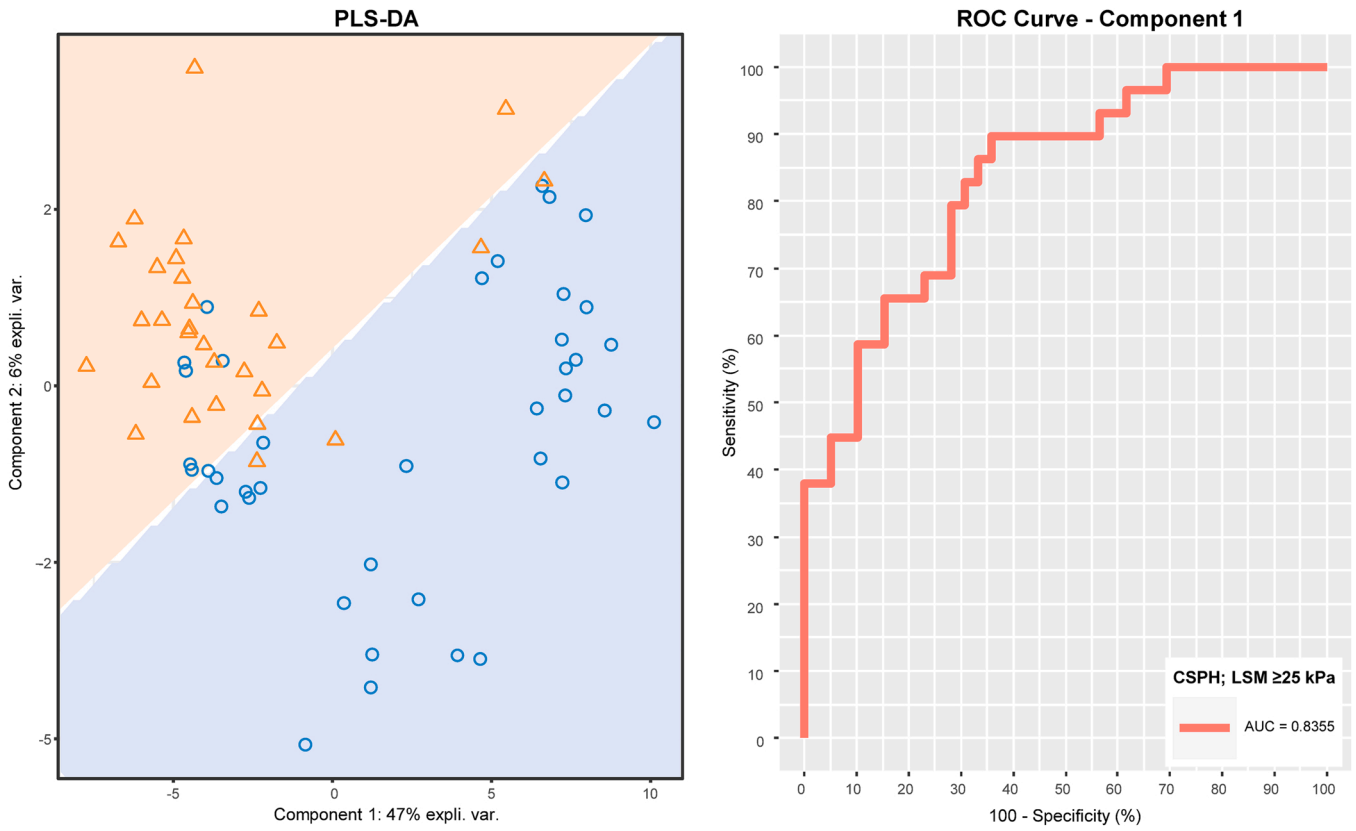

Fig. 2. Multivariate analysis of 60 SDE transcripts from PBMCs to discriminate advanced cirrhosis with high risk for clinically significant portal hypertension (CSPH) in HIV/HCV coinfected patients. A) The partial least squares discriminant analysis (PLS-DA) plot can differentiate patients with ≥ 25 kPa (orange triangles) from patients with < 25 kPa (blue circles). B) The area under the receiver operating characteristic curve (AUROC) estimates an excellent PLS-DA classification performance. Statistics: Multivariate analysis was performed by PLS-DA, a ROC curve was plotted, and AUROC was calculated. Abbreviations: PLS-DA, Partial least squares discriminant analysis; ROC, Receiver operating characteristic; AUROC, Area under the ROC.

Table 2
Summary of predictive performance and odds of peripheral blood gene expression (counts) for advanced cirrhosis with high risk for clinically significant portal hypertension ((<25 kPa (n = 39) vs. ≥ 25 kPa (n = 29)) in HIV/HCV-coinfected individuals.

	AUROC	95%CI	OR	95%CI	*p*-value
TMEM64	0.752	0.636 – 0.867	1.25	1.09 – 1.43	0.001
SCAMP1	0.753	0.631 – 0.874	1.15	1.06 – 1.26	0.001
GPR146	0.756	0.640 – 0.873	1.93	1.28 – 2.91	0.002
GTF2A1	0.772	0.652 – 0.891	1.11	1.05 – 1.19	0.001
ABHD17B	0.776	0.658 – 0.893	1.13	1.06 – 1.21	0.001
ZFHX2-AS1	0.791	0.684 – 0.898	0.50	0.34 – 0.74	< 0.001
MDK	0.793	0.682 – 0.905	0.21	0.08 – 0.52	0.001
STAG3L2	0.794	0.684 – 0.904	0.30	0.16 – 0.57	< 0.001

Statistic: Values are expressed as the area under the curve ROC (AUROC), odds ratio (OR), and 95% confidence interval (95%CI).
Abbreviations. HCV, hepatitis C virus; HIV, human immunodeficiency virus.

marker of HCC in patients with HCV-related cirrhosis, but the role of *MDK* before the HCC apparition is much less studied. MDK may be induced at earlier fibrosis stages to protect liver cells from ongoing aggression [57]. Fibrosis progression could alter *MDK* function and expression, which may be related to the cirrhosis-associated immune dysfunction characteristic of cirrhotic patients [8]. During the early HCC stage, *MDK* expression would be induced by hypoxia in the tumor microenvironment, and its anti-apoptotic functions would contribute to carcinogenesis instead [58]. Our study found that *MDK* expression decreases as liver cirrhosis increases, supporting the dual function of *MDK* as a liver protector and carcinogenesis promoter. Interestingly, *MDK* expression in a model of lung fibrosis was shown to be biphasic, with increased expression in both the early and late stages of fibrosis [59].

This set of SDE transcripts showed excellent discriminative ability for advanced cirrhosis with a high risk for CSPH (≥ 25 kPa). However, SDE transcripts to identify patients with advanced cirrhosis with increased risk for CSPH may be of little practical use since the physical examination and abdominal ultrasound make advanced cirrhosis easy to detect in the clinical setting. Despite that, omics-based analyses are becoming more accessible, and their routine application at the clinical level is closer than ever. Moreover, our study addresses two main purposes at this point. Firstly, our findings can help to understand the pathophysiological mechanisms underlying fibrosis progression and portal hypertension development at this disease stage. Secondly, it suggests molecular targets that can be employed for diagnostic or therapeutic applications. These findings could help explain the variability and the appearance of complications in advanced chronic liver disease and allow individualized management of these patients, improving the outcome of this disease.

4.1. Limitations of the study

Our study has some limitations that should be taken into account. Firstly, our sample size may limit the statistical power to detect minor differences between groups and increase the risk of false-positive results. Secondly, the lack of liver biopsies to assess the grade of fibrosis since the practice of liver biopsies in Spain is no longer in use. However, although liver biopsy was considered the gold standard, its role as a gold standard is far from perfect because it has several drawbacks regarding constrained feasibility, complications that can arise during the procedure, and sampling errors [13]. Moreover, transient elastography is validated in HIV/HCV coinfected patients to measure liver stiffness [60].

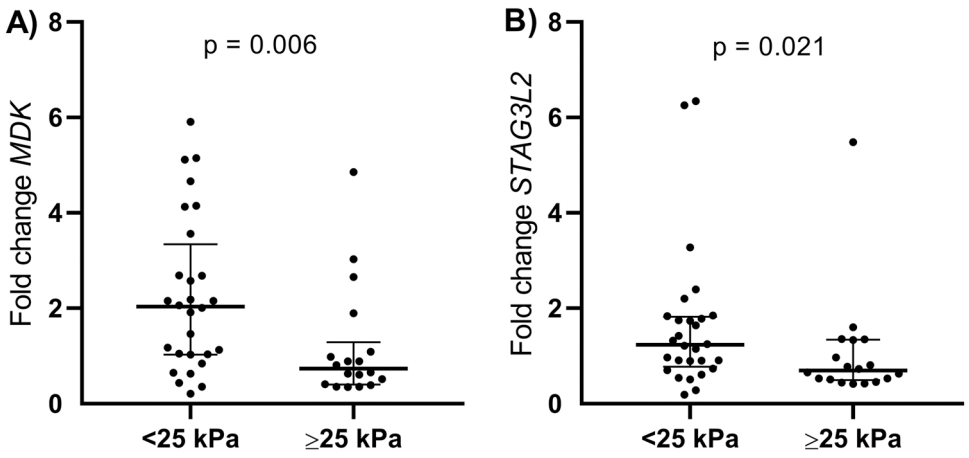

Fig. 3. Validation by RT-qPCR of differences in *MDK* (A) and *STAG3L2* (B) gene expression for advanced cirrhosis with high risk for clinically significant portal hypertension (CSPH) (LSM ≥25 kPa). Relative quantification is expressed as n-fold relative to the calibrator sample. Statistics: The *p*-values were estimated using the Mann-Whitney test. Abbreviations: MDK, Midkine; STAG3L2, Stromal antigen 3-like 2; kPa, Kilopascals.

Thirdly, hepatic venous pressure gradient measurement (HPVG) remains the gold standard for the diagnosis of CSPH, as recommended in the Baveno VII Consensus [13–15]. Thus, emerging biomarkers to discriminate between CSPH and non-CSPH status should be compared with the HPVG. This comparison would have reinforced our findings, but the data scarcity in our study precluded its assessment (HPVG data available in only 15 patients of the ESCORIAL cohort, 5 of them with HVPG values ≤10 mmHg). Nevertheless, Baveno VII also aimed for a pragmatic definition of cACLD based on transient elastography [13–15], considering that non-invasive tests are sufficiently accurate to identify CSPH in clinical practice. In this regard, our study delves into the underlying molecular differences between patients with and without advanced cirrhosis with high risk for CSPH, finding several transcripts with high discrimination ability in the two independent cohorts studied.

5. Conclusions

A gene expression signature of 60 SDE transcripts was related to advanced cirrhosis with high risk for CSPH in HIV/HCV coinfected patients. Of these, *MDK* and *STAG3L2* were validated and showed good discriminative value. Our data may help clarify the pathophysiological mechanisms involved in advanced cirrhosis in this population group. Further studies and longitudinal data are required to delve into the biological meaning of these findings.

Ethics approval and consent to participate

This study was carried out according to the Declaration of Helsinki and was approved by the Research Ethics Committee of the Instituto de Salud Carlos III (CEI PI 23_2011 and CEI PI 41_2014). Written informed consent was obtained from all participants in the study.

Funding

This study was supported by grants from Instituto de Salud Carlos III (ISCIII; grant numbers CP17CIII/00007 and PI18CIII/00028 to MAJS, PI17/00657 and PI20/00474 to JB, PI17/00903 and PI20/00507 to JGG, PI18CIII/00020 to AFR, and PI17CIII/00003 and PI20CIII/00004 to SR) and Ministerio de Ciencia e Innovación (AEI, PID2021-126781OB-I00 to AFR). The study was also funded by the CIBER -Consorcio Centro de Investigación Biomédica en Red- (CB 2021), Instituto de Salud Carlos III, Ministerio de Ciencia e Innovación and Unión Europea – NextGenerationEU (CB21/13/00044).

Consent for publication

Not applicable.

Author contributions

Conceptualization: SR and MAJS. Data curation: JB, JGG, CD, VH, and LPLT. Formal analysis: SS, OBK, SR, MAJS, and AFR. Funding acquisition: JB, JGG, MAJS, and SR. Investigation and methodology: SS, OBK, AFR, and AVB. Project Administration: JB. Supervision and visualization: SR. Writing – original draft preparation: AFR, MAJS, and SR. Writing – review & editing: IM. All authors have read and approved the final manuscript.

Competing interests

The authors declare that they have no competing interests.

Acknowledgments

We particularly want to acknowledge the patients in this study for their participation, the Spanish HIV HGM BioBank, and the collaborating Centers for the generous gifts of clinical samples used in this work. We also thank the Bioinformatics Unit at the Institute of Health Carlos III for their valuable support for the bioinformatics analysis.

Authors' information

Not applicable.

Appendix

The GESIDA 3603b Cohort Study Group

Hospital General Universitario Gregorio Marañón, Madrid: A Carrero, P Miralles, JC López, F Parras, B Padilla, T Aldamiz-Echevarría, F Tejerina, C Díez, L Pérez-Latorre, C Fanciulli, I Gutiérrez, M Ramírez, S Carretero, JM Bellón, J Bermejo, and J Berenguer.

Hospital Universitario La Paz, Madrid: V Hontañón, JR Arribas, mL Montes, I Bernardino, JF Pascual, F Zamora, JM Peña, F Arnalich, M Díaz, J González-García.

Hospital de la Santa Creu i Sant Pau, Barcelona: P Domingo, JM Guardiola.

Hospital Universitari Vall d'Hebron, Barcelona: E Van den Eynde,

M Pérez, E Ribera, M Crespo.

Hospital Universitario Ramón y Cajal, Madrid: JL Casado, F Dronda, A Moreno, MJ Pérez-Elías, MA Sanfrutos, S Moreno, C Quereda.

Hospital Universitario Príncipe de Asturias, Alcalá de Henares: A Arranz, E Casas, J de Miguel, S Schroeder, J Sanz.

Hospital Universitario de La Princesa, Madrid: J Sanz, I Santos.

Hospital Donostia, San Sebastián: MJ Bustinduy, JA Iribarren, F Rodríguez-Arrondo, MA Von-Wichmann.

Hospital Clínico San Carlos, Madrid: J Vergas, MJ Téllez.

Hospital Universitario San Cecilio, Granada: D. Vinuesa, L. Muñoz, and J. Hernández-Quero.

Hospital Clínico Universitario, Valencia: A Ferrer, MJ Galindo.

Hospital General Universitario, Valencia: L Ortiz, E Ortega.

Hospital Universitari La Fe, Valencia: M Montero, M Blanes, S Cuellar, J Lacruz, M Salavert, J López-Aldeguer.

Hospital Universitario de Getafe, Getafe: G Pérez, G Gaspar.

Fundación SEIMC-GESIDA, Madrid: M Yllescas, P Crespo, E Aznar, H Esteban.

The ESCORIAL study group

Hospital General Universitario Gregorio Marañón (Madrid, Spain): Cristina Díez, Luis Ibáñez, Leire Pérez-Latorre, Diego Rincón, Teresa Aldámiz-Echevarría, Vega Catalina, Pilar Miralles, Teresa Aldámiz-Echevarría, Francisco Tejerina, María C Gómez-Rico, Esther Alonso, José M Bellón, Rafael Bañares, and Juan Berenguer.

Hospital Universitario La Paz/IdiPAZ (Madrid, Spain): José Arribas, José I Bernardino, Ana Delgado, Carmen Busca, Javier García-Samaniego, Víctor Hontañón, Luz Martín-Carbonero, Rafael Micán, María L Montes-Ramírez, Victoria Moreno, Antonio Olveira, Ignacio Pérez-Valero, Eulalia valencia, and Juan González-García.

Hospital Universitario Puerta de Hierro (Madrid, Spain): Elba Llop and José Luis Calleja.

Hospital Universitario Ramón y Cajal (Madrid, Spain): Javier Martínez and Agustín Albillos.

Fundación SEIMC/GeSIDA (Madrid, Spain): Marta de Miguel, María Yllescas, and Herminia Esteban.

References

[1] The Polaris Observatory HCV Collaborators, Global prevalence and genotype distribution of hepatitis C virus infection in 2015: a modelling study, Lancet Gastroenterol. Hepatol. 2 (3) (2017) 161–176.

[2] B. Hajarizadeh, J. Grebely, G.J. Dore, Epidemiology and natural history of HCV infection, Nat. Rev. Gastroenterol. Hepatol. 10 (9) (2013) 553–562.

[3] A. Vallet-Pichard, S. Pol, Natural history and predictors of severity of chronic hepatitis C virus (HCV) and human immunodeficiency virus (HIV) co-infection, J. Hepatol. 44 (1 Suppl) (2006) S28–S34.

[4] P. Ingiliz, J.K. Rockstroh, Natural history of liver disease and effect of hepatitis C virus on HIV disease progression, Curr. Opin. HIV AIDS 10 (5) (2015) 303–308.

[5] V. Hernandez-Gea, S.L. Friedman, Pathogenesis of liver fibrosis, Annu. Rev. Pathol.: Mech. Dis. 6 (1) (2011) 425–456.

[6] S.K. Asrani, P.S. Kamath, Natural history of cirrhosis, Curr. Gastroenterol. Rep. 15 (2) (2013) 308.

[7] L.M. Medrano, P. Garcia-Broncano, J. Berenguer, J. Gonzalez-Garcia, M. A. Jimenez-Sousa, J.M. Guardiola, M. Crespo, C. Quereda, J. Sanz, I. Canorea, A. Carrero, V. Hontanon, M.A. Munoz-Fernandez, S. Resino, G.B.S. Group, Elevated liver stiffness is linked to increased biomarkers of inflammation and immune activation in HIV/hepatitis C virus-coinfected patients, Aids 32 (9) (2018) 1095–1105.

[8] A. Albillos, R. Martin-Mateos, S. Van der Merwe, R. Wiest, R. Jalan, M. Álvarez-Mon, Cirrhosis-associated immune dysfunction, Nat. Rev. Gastroenterol. Hepatol. 19 (2) (2022) 112–134.

[9] M.G. Refolo, C. Messa, V. Guerra, B.I. Carr, R. D'Alessandro, Inflammatory mechanisms of HCC development, Cancers 12 (3) (2020).

[10] S.J. Polyak, I.N. Crispe, T.F. Baumert, Liver abnormalities after elimination of HCV infection: persistent epigenetic and immunological perturbations post-cure, Pathogens 10 (1) (2021) 44.

[11] J. Berenguer, I. Jarrín, L. Pérez-Latorre, V. Hontañón, M.J. Vivancos, J. Navarro, M.J. Téllez, J.M. Guardiola, J.A. Iribarren, A. Rivero-Juárez, M. Márquez, A. Artero, L. Morano, I. Santos, J. Moreno, M.C. Fariñas, M.J. Galindo, M. A. Hernando, M. Montero, C. Cifuentes, P. Domingo, J. Sanz, L. Domíngez, O. L. Ferrero, B. De la Fuente, C. Rodríguez, S. Reus, J. Hernández-Quero, G. Gaspar, L. Pérez-Martínez, C. García, L. Force, S. Veloso, J.E. Losa, J. Vilaró, E. Bernal, S. Arponen, A.J. Ortí, Á. Chocarro, R. Teira, G. Alonso, R. Silvariño, A. Vegas, P. Geijo, J. Bisbe, H. Esteban, J. González-García, S.S.G. Ge, Human immunodeficiency virus/hepatits C virus coinfection in spain: elimination is feasible, but the burden of residual cirrhosis will be significant, Open Forum Infect. Dis. 5 (1) (2018) ofx258.

[12] A.J. Jeyarajan, R.T. Chung, Insights into the pathophysiology of liver disease in HCV/HIV: does it end with HCV cure? J. Infect. Dis. 222 (Suppl 9) (2020) S802–s813.

[13] L. Castera, X. Forns, A. Alberti, Non-invasive evaluation of liver fibrosis using transient elastography, J. Hepatol. 48 (5) (2008) 835–847.

[14] G. Garcia-Tsao, J.G. Abraldes, A. Berzigotti, J. Bosch, Portal hypertensive bleeding in cirrhosis: risk stratification, diagnosis, and management: 2016 practice guidance by the American Association for the study of liver diseases, Hepatology 65 (1) (2017) 310–335.

[15] R. de Franchis, J. Bosch, G. Garcia-Tsao, T. Reiberger, C. Ripoll, Baveno VII - Renewing consensus in portal hypertension, J. Hepatol. 76 (4) (2022) 959–974.

[16] J. Lambrecht, S. Verhulst, I. Mannaerts, H. Reynaert, L.A. van Grunsven, Prospects in non-invasive assessment of liver fibrosis: Liquid biopsy as the future gold standard? Biochim. Biophys. Acta BBA Mol. Basis Dis. 1864 (4, Part A) (2018) 1024–1036.

[17] A. Minutolo, B. Conti, S. Grelli, C. Viscomi, G. Labbadia, C. Balsano, Lymphocytes as liver damage mirror of HCV related adipogenesis deregulation, PLoS One 9 (3) (2014), e92343.

[18] J. Mann, H.L. Reeves, A.E. Feldstein, Liquid biopsy for liver diseases, Gut 67 (12) (2018) 2204–2212.

[19] Y. Hoshida, A. Villanueva, A. Sangiovanni, M. Sole, C. Hur, K.L. Andersson, R. T. Chung, J. Gould, K. Kojima, S. Gupta, B. Taylor, A. Crenshaw, S. Gabriel, B. Minguez, M. Iavarone, S.L. Friedman, M. Colombo, J.M. Llovet, T.R. Golub, Prognostic gene expression signature for patients with hepatitis C-related early-stage cirrhosis, Gastroenterology 144 (5) (2013) 1024–1030.

[20] H. Takeda, A. Takai, E. Iguchi, M. Mishima, S. Arasawa, K. Kumagai, Y. Eso, T. Shimizu, K. Takahashi, Y. Ueda, K. Taura, E. Hatano, H. Iijima, H. Aoyagi, H. Aizaki, H. Marusawa, T. Wakita, H. Seno, Oncogenic transcriptomic profile is sustained in the liver after the eradication of the hepatitis C virus, Carcinogenesis 42 (5) (2021) 672–684.

[21] B. Ijaz, W. Ahmad, T. Das, K. Shabbiri, T. Husnain, S. Hassan, HCV infection causes cirrhosis in human by step-wise regulation of host genes involved in cellular functioning and defense during fibrosis: Identification of bio-markers, Genes Dis. 6 (3) (2019) 304–317.

[22] A. Whitmill, S. Kim, V. Rojas, F. Gulraiz, K. Afreen, M. Jain, M. Singh, I.-W. Park, Signature molecules expressed differentially in a liver disease stage-specific manner by HIV-1 and HCV co-infection, PLoS One 13 (8) (2018), e0202524.

[23] A. Jangra, A. Kothari, P. Sarma, B. Medhi, B.J. Omar, K. Kaushal, Recent advancements in antifibrotic therapies for regression of liver fibrosis, Cells 11 (9) (2022) 1500.

[24] P. Garcia-Broncano, L.M. Medrano, J. Berenguer, O. Brochado-Kith, J. González-García, M.Á. Jiménez-Sousa, C. Quereda, J. Sanz, M.J. Téllez, L. Díaz, J.L. JImenez, S. Resino, GESIDA 3603b Study Group, Mild profile improvement of immune biomarkers in HIV/HCV-coinfected patients who removed hepatitis C after HCV treatment: A prospective study, J Infect. 80 (1) (2020) 99–110, https://doi.org/10.1016/j.jinf.2019.09.020. Epub 2019 Oct 1.PMID: 31585189.

[25] S. Salguero, L.M. Medrano, J. Gonzalez-Garcia, J. Berenguer, M.L. Montes, C. Diez, P. Garcia-Broncano, E. Llop-Herrera, L. Perez-Latorre, J.M. Bellono, M.A. Jimenez-Sousa, S. Resino, Plasma IP-10 and IL-6 are linked to Child-Pugh B cirrhosis in patients with advanced HCV-related cirrhosis: a cross-sectional study, Sci. Rep. 10 (1) (2020) 10384.

[26] O. Brochado, I. Martinez, J. Berenguer, L. Medrano, J. Gonzalez-Garcia, M. A. Jimenez-Sousa, A. Carrero, V. Hontanon, J. Navarro, J.M. Guardiola, A. Fernandez-Rodriguez, S. Resino, G.S. Group, HCV eradication with IFN-based therapy does not completely restore gene expression in PBMCs from HIV/HCV-coinfected patients, J. Biomed. Sci. 28 (1) (2021) 23.

[27] A.L. Rasmussen, I.M. Wang, M.C. Shuhart, S.C. Proll, Y. He, R. Cristescu, C. Roberts, V.S. Carter, C.M. Williams, D.L. Diamond, J.T. Bryan, R. Ulrich, M. J. Korth, L.V. Thomassen, M.G. Katze, Chronic immune activation is a distinguishing feature of liver and PBMC gene signatures from HCV/HIV coinfected patients and may contribute to hepatic fibrogenesis, Virology 430 (1) (2012) 43–52.

[28] S. Listopad, C. Magnan, A. Asghar, A. Stolz, J.A. Tayek, Z.X. Liu, T.R. Morgan, T. M. Norden-Krichmar, Differentiating between liver diseases by applying multiclass machine learning approaches to transcriptomics of liver tissue or blood-based samples, JHEP Rep. 4 (10) (2022), 100560.

[29] Z. He, D. Yang, X. Fan, M. Zhang, Y. Li, X. Gu, M. Yang, The roles and mechanisms of lncRNAs in liver fibrosis, Int. J. Mol. Sci. 21 (4) (2020) 1482.

[30] T. Meier, M. Timm, M. Montani, L. Wilkens, Gene networks and transcriptional regulators associated with liver cancer development and progression, BMC Med. Genom. 14 (1) (2021) 41.

[31] C. Schrenk, V. Fetz, C. Vallet, C. Heiselmayer, E. Schröder, A. Hensel, A. Hahlbrock, D. Wünsch, D. Goesswein, C. Bier, N. Habtemichael, G. Schneider, R.H. Stauber, S. K. Knauer, TFIIA transcriptional activity is controlled by a 'cleave-and-run' Exportin-1/Taspase 1-switch, J. Mol. Cell Biol. 10 (1) (2017) 33–47.

[32] J. Jiang, B. Liu, R. Liu, W. Yang, Overexpression of taspase 1 predicts poor prognosis in patients with hepatocellular carcinoma, Cancer Manag. Res. 13 (2021) 2517–2537.

[33] A. Castle, D. Castle, Ubiquitously expressed secretory carrier membrane proteins (SCAMPs) 1-4 mark different pathways and exhibit limited constitutive trafficking to and from the cell surface, J. Cell Sci. 118 (Pt 16) (2005) 3769–3780.

[34] D. Spano, A. Colanzi, Golgi complex: a signaling hub in cancer, Cells 11 (13) (2022).
[35] S. Sung, J. Kim, Y. Jung, Liver-derived exosomes and their implications in liver pathobiology, Int. J. Mol. Sci. 19 (12) (2018).
[36] X. Zhang, J. Sheng, Y. Zhang, Y. Tian, J. Zhu, N. Luo, C. Xiao, R. Li, Overexpression of SCAMP3 is an indicator of poor prognosis in hepatocellular carcinoma, Oncotarget 8 (65) (2017) 109247–109257.
[37] A.R. Owens, C.E. McInerney, K.M. Prise, D.G. McArt, A. Jurek-Loughrey, Novel deep learning-based solution for identification of prognostic subgroups in liver cancer (Hepatocellular carcinoma), BMC Bioinforma. 22 (1) (2021) 563.
[38] C.G. Miao, Y.Y. Yang, X. He, C. Huang, Y. Huang, L. Zhang, X.W. Lv, Y. Jin, J. Li, Wnt signaling in liver fibrosis: progress, challenges and potential directions, Biochimie 95 (12) (2013) 2326–2335.
[39] A.M. Khalaf, D. Fuentes, A.I. Morshid, M.R. Burke, A.O. Kaseb, M. Hassan, J. D. Hazle, K.M. Elsayes, Role of Wnt/β-catenin signaling in hepatocellular carcinoma, pathogenesis, and clinical significance, J. Hepatocell. Carcinoma 5 (2018) 61–73.
[40] H. Kim, T. Kim, B.-C. Jeong, I.-T. Cho, D. Han, N. Takegahara, T. Negishi-Koga, H. Takayanagi, J.H. Lee, J.-Y. Sul, V. Prasad, S.H. Lee, Y. Choi, Tmem64 modulates calcium signaling during RANKL-mediated osteoclast differentiation, Cell Metab. 17 (2) (2013) 249–260.
[41] V. Brucklacher-Waldert, C. Ferreira, M. Stebegg, O. Fesneau, S. Innocentin, J. C. Marie, M. Veldhoen, Cellular stress in the context of an inflammatory environment supports TGF-β-independent T helper-17 differentiation, Cell Rep. 19 (11) (2017) 2357–2370.
[42] P. Garcia-Broncano, L.M. Medrano, J. Berenguer, J. González-García, M.Á. Jiménez-Sousa, A. Carrero, V. Hontañón, J.M. Guardiola, M. Crespo, C. Quereda, J. Sanz, A.B. García-Gómez, J.L. Jimenez, S. Resino, G.b.S. group, dysregulation of the immune system in HIV/HCV-coinfected patients according to liver stiffness status, Cells 7 (11) (2018) 196.
[43] C.E. Coronel-Castillo, X. Qi, J. Contreras-Carmona, O.L. Ramirez-Perez, N. Mendez-Sanchez, Nonalcoholic fatty liver disease and nonalcoholic steatohepatitis in HIV infection: a metabolic approach of an infectious disease, Expert Rev. Gastroenterol. Hepatol. 13 (6) (2019) 531–540.
[44] H. Huang, N. Zhang, Q. Xiong, R. Chen, C. Zhang, N. Wang, L. Wang, H. Ren, M. Liu, M. Qian, B. Du, Elimination of GPR146-mediated antiviral function through IRF3/HES1-signalling pathway, Immunology 152 (1) (2017) 102–114.
[45] H. Yu, A. Rimbert, A.E. Palmer, T. Toyohara, Y. Xia, F. Xia, L.M.R. Ferreira, Z. Chen, T. Chen, N. Loaiza, N.B. Horwitz, M.C. Kacergis, L. Zhao, B. Consortium, A.A. Soukas, J.A. Kuivenhoven, S. Kathiresan, C.A. Cowan, GPR146 deficiency protects against hypercholesterolemia and atherosclerosis, Cell 179 (6) (2019) 1276–1288, e14.
[46] B.C. Jeong, T.S. Kim, H.S. Kim, S.H. Lee, Y. Choi, Transmembrane protein 64 reciprocally regulates osteoblast and adipocyte differentiation by modulating Wnt/β-catenin signaling, Bone 78 (2015) 165–173.
[47] N. Rocha, F. Payne, I. Huang-Doran, A. Sleigh, K. Fawcett, C. Adams, A. Stears, V. Saudek, S. O'Rahilly, I. Barroso, R.K. Semple, The metabolic syndrome-associated small G protein ARL15 plays a role in adipocyte differentiation and adiponectin secretion, Sci. Rep. 7 (1) (2017) 17593.
[48] V.S. Naumenko, E. Ponimaskin, Palmitoylation as a functional regulator of neurotransmitter receptors, Neural Plast. 2018 (2018) 5701348.
[49] S. Mathew, M. Faheem, S.M. Ibrahim, W. Iqbal, B. Rauff, K. Fatima, I. Qadri, Hepatitis C virus and neurological damage, World J. Hepatol. 8 (12) (2016) 545–556.
[50] Q.-t Chen, Z.-y Zhang, Q.-l Huang, H. Chen, W.-b Hong, T. Lin, C.-y Ju, L.-z Wu, Y.-y Huang, P. Hou, W.-j Wang, X.-m Deng, Q. Wu, Intercellular communication in the progression from fibrosis to HCC by ectosomal HK1-induced TGF-β secretion, SSRN Electron. J. (2021).
[51] S. Salguero, D. Rojo, J. Berenguer, J. Gonzalez-Garcia, A. Fernandez-Rodriguez, O. Brochado-Kith, C. Diez, V. Hontanon, A. Virseda-Berdices, J. Martinez, L. Ibanez-Samaniego, E. Llop-Herrera, C. Barbas, S. Resino, M.A. Jimenez-Sousa, G. Escorial, Study, Plasma metabolomic fingerprint of advanced cirrhosis stages among HIV/HCV-coinfected and HCV-monoinfected patients, Liver Int. 40 (9) (2020) 2215–2227.
[52] A.M. Habib, A. Matsuyama, A.L. Okorokov, S. Santana-Varela, J.T. Bras, A. M. Aloisi, E.C. Emery, Y.D. Bogdanov, M. Follenfant, S.J. Gossage, M. Gras, J. Humphrey, A. Kolesnikov, K. Le Cann, S. Li, M.S. Minett, V. Pereira, C. Ponsolles, S. Sikandar, J.M. Torres, K. Yamaoka, J. Zhao, Y. Komine, T. Yamamori, N. Maniatis, K.I. Panov, H. Houlden, J.D. Ramirez, D.L.H. Bennett, L. Marsili, V. Bachiocco, J.N. Wood, J.J. Cox, A novel human pain insensitivity disorder caused by a point mutation in ZFHX2, Brain 141 (2) (2018) 365–376.
[53] S. Munkgaard, H. Kelbaek, B. Tronier, Elevated plasma somatostatin in cirrhosis of the liver, New Engl. J. Med. 304 (23) (1981) 1429–1430.
[54] G.C, The Genotype-Tissue Expression (GTEx) project, Nat. Genet 45 (6) (2013) 580–585.
[55] J.N. Weinstein, E.A. Collisson, G.B. Mills, K.R. Shaw, B.A. Ozenberger, K. Ellrott, I. Shmulevich, C. Sander, J.M. Stuart, The Cancer Genome Atlas Pan-Cancer analysis project, Nat. Genet 45 (10) (2013) 1113–1120.
[56] Y.Q. Cai, Y. Lv, Z.C. Mo, J. Lei, J.L. Zhu, Q.Q. Zhong, Multiple pathophysiological roles of midkine in human disease, Cytokine 135 (2020), 155242.
[57] N. Yazihan, H. Ataoglu, E. Akcil, B. Yener, B. Salman, C. Aydin, Midkine secretion protects Hep3B cells from cadmium induced cellular damage, World J. Gastroenterol. 14 (1) (2008) 76–80.
[58] A. Gowhari Shabgah, F. Ezzatifar, S. Aravindhan, A. Olegovna Zekiy, M. Ahmadi, S. M. Gheibihayat, J. Gholizadeh Navashenaq, Shedding more light on the role of Midkine in hepatocellular carcinoma: new perspectives on diagnosis and therapy, IUBMB Life 73 (4) (2021) 659–669.
[59] K. Misa, Y. Tanino, X. Wang, T. Nikaido, M. Kikuchi, Y. Sato, R. Togawa, M. Tanino, S. Tanaka, K. Kadomatsu, M. Munakata, Involvement of midkine in the development of pulmonary fibrosis, Physiol. Rep. 5 (16) (2017).
[60] S. Resino, M. Sanchez-Conde, J. Berenguer, Coinfection by human immunodeficiency virus and hepatitis C virus: noninvasive assessment and staging of fibrosis, Curr. Opin. Infect. Dis. 25 (5) (2012) 564–569.